ELSEVIER

International Journal of Minerals, Metallurgy and Materials
Volume 16, Number 4, August 2009, Page 387

Materials

Fabrication of high nitrogen austenitic stainless steels with excellent mechanical and pitting corrosion properties

Hua-bing Li, *Zhou-hua Jiang*, *Yang Cao*, *and Zu-rui Zhang*

School of Materials and Metallurgy, Northeastern University, Shenyang 110004, China
(Received 2008-08-14)

Abstract: A series of high nitrogen austenitic stainless steels were successfully developed with a pressurized electroslag remelting furnace. Nitride additives and deoxidizer were packed into the stainless steel pipes, and then the stainless steel pipes were welded on the surface of an electrode with low nitrogen content to prepare a compound electrode. Using Si_3N_4 as a nitrogen alloying source, the silicon contents in the ingots were prone to be out of the specification range, the electric current fluctuated greatly and the surface qualities of the ingots were poor. The surface qualities of the ingots were improved with FeCrN as a nitrogen alloying source. The sound and compact macrostructure ingot with the maximum nitrogen content of 1.21wt% can be obtained. The 18Cr18Mn2Mo0.9N high nitrogen austenitic stainless steel exhibits high strength and good ductility at room temperature. The steel shows typical ductile-brittle transition behavior and excellent pitting corrosion resistance properties.

Key words: high nitrogen austenitic stainless steels; electroslag remelting; nitrogen alloying; ductile-brittle transition; pitting corrosion resistance

[*The work was financially supported by the National Natural Science Foundation of China (No.50534010).*]

1. Introduction

High nitrogen stainless steels (HNS), particularly high nitrogen austenitic stainless steels, are becoming an increasingly important new class of engineering material because of their mechanical and corrosion resistance properties, which are surprisingly improved by the addition of nitrogen [1-2]. Furthermore, nitrogen as a stronger austenite stabilizer in austenitic stainless steels can replace expensive nickel, which is allergic to human bodies. Owing to the above beneficial effects of nitrogen, nitrogen-alloyed stainless steels are applied in the power-generating industry, ship building, railway, chemical equipment, biomaterial, and petroleum industry. Since 1988, the international conferences on HNS held successively for eight times greatly promote the development of HNS in the world. In recent years, more than 10 HNS research groups in Chinese universities, research institutes, and also steel companies carried out several research works concerning the structure, manufacture, properties, and applications of nitrogen-alloyed steels [3-8]. However, the development of nitrogen alloying stainless steels, especially HNS for industrial scale, has been limited greatly in China due to shortage of key manufacture equipments and technologies.

In the present work, high nitrogen austenitic stainless steels were attempted to manufacture by pressurized electroslag remelting. The methods of nitrogen alloying and deoxidization were investigated to obtain the suitable process under high nitrogen pressure. The chemical composition of the ingots was analyzed to examine the homogeneous distribution of nitrogen. Hot acid etching was carried out for determining the macrostructure of the ingots. The mechanical and pitting corrosion resistance properties of high nitrogen austenitic stainless steel were also investigated.

2. Experimental

The manufacture of high nitrogen austenitic stainless steels was attempted using a 50-kg pressurized electroslag remelting furnace with an advanced

Corresponding author: Hua-bing Li, **E-mail:** lihb@smm.neu.edu.cn
Also available online at www.sciencedirect.com

control system as shown in Fig. 1. A device was invented to assure the dynamic pressure equalization between the melting chamber and the cooling water system. The maximum nitrogen pressure could arrive at 7 MPa. The electrodes with low nitrogen content were prepared by a vacuum induction furnace (VIF) under nitrogen atmosphere. Nitride additives (FeCrN, Si_3N_4) and deoxidizer (FeSi, CaSi, Si_3N_4) were packed into the stainless steel pipes, and then the stainless steels pipes were welded on the surface of an electrode to prepare a compound electrode. The two slag systems with ANF-6 and 63wt%CaF_2-17wt%CaO-15wt%Al_2O_3-2wt%SiO_2-3wt%MgO were chosen for the pressurized electroslag remelting process.

Fig. 1. 50-kg pressurized electroslag remelting furnace with 7 MPa maximum pressure.

The heat 18Cr18Mn2MoN with 0.93wt% nitrogen (18Cr18Mn2Mo0.9N) was hot rolled, and solution treatment was performed at 1150°C for 30 min followed by quenching with water. Then, the steels were all cold rolled to about 1.5 mm in thickness. The cold rolled steels were all annealed at 1150°C for 30 min followed by water quenching. The dimensions of the V-notched Charpy specimens were 7.5 mm in thickness, 10 mm in width, and 55 mm in length. The tensile tests of all the specimens were performed with different crosshead speeds at room temperature (RT). The impact property test of the steel was also performed under the temperature from 77 K to RT. The anodic polarization curves of 18Cr18Mn2Mo0.9N were carried out in the 3.5wt% NaCl with pH values ranging from 1 to 5. The pH values of the solution were adjusted by adding HCl and NaOH. All measurements were carried out using a potentiostat PARSTAT 2273, which was comprised of three electrodes. A platinum foil and a saturated calomel electrode (SCE) were used as the counter and reference electrodes, respectively. The scan rates in the above experiments were all controlled at 20 mV/min. The solution was deaerated with high purity nitrogen before testing for half an hour and kept under nitrogen atmosphere during testing. A type of 316L stainless steel was also included for comparison purpose. The specimens of 10 mm×10 mm×3 mm for investigation were machined from the hot rolled sheets. All the specimens were solution annealed at 1150°C for 30 min followed by water quenching.

3. Results and discussion

3.1. Manufacture of high nitrogen steels by pressurized electroslag remelting

The high nitrogen austenitic stainless steels were manufactured using a pressurized electroslag remelting furnace by different nitrogen alloying sources and deoxidizers as shown in Table 1.

Table 1. Nitrogen source, nitrogen pressure, deoxidizer, and nitrogen content in electrodes

No.	Initial nitrogen in electrodes made by vacuum induction melting (VIM) / wt%	Pressure / MPa	Nitrided alloys	Deoxidizer	Mass of deoxidizer / g
1	0.56	2.0	FeCrN	FeSi	70
2	0.53	2.1	FeCrN	FeSi	80
3	0.57	2.1	FeCrN	FeSi	90
4	0.57	2.5	FeCrN	FeSi	130
5	0.43	3.0	FeCrN	CaSi, Si_3N_4	100, 70
6	0.53	3.0	FeCrN and Si_3N_4	CaSi	60
7	0.51	3.1	Si3N4	CaSi	120
8	0.30	3.2	FeCrN	CaSi	100

The chemical composition of high nitrogen austenitic stainless steels manufactured with a pressurized electro-slag remelting (ESR) furnace is shown in Table 2. The nitrogen contents in the ingots were in the range of 0.63wt% to 1.21wt%. In order to investigate the effect of nitrogen pressure on the nitrogen content of ESR ingots, the heat No.3 and No.4 with the same initial nitrogen in electrodes and using the same amount FeCrN alloys were remelted under the nitrogen pressures of 2.1 MPa and 2.5 MPa, respectively. But there was no change of the nitrogen content in the heat No.3 and No.4 ESR ingots. The results indicated that the nitrogen content in ESR ingots mainly depended on the initial nitrogen in electrodes and the

amount of nitrided alloys. Massive nitrogen alloying in the pressurized electroslag remelting process did not take place *via* gas phase. Owing to the extremely short dwelling time of the metal droplets in the liquid phase and the resultant absent of equilibrium conditions, nitrogen pick-up *via* nitrogen-rich atmosphere was negligible [9]. The nitrogen pressure in the furnace served to retain the nitrogen in the nitrided alloy into the molten metal and prevent from the formation of nitrogen gas pores during the solidification of the ESR ingots. The oxygen contents were lightly higher except for the heat No.7, so it was necessary to investigate the suitable deoxidization method during the pressurized electroslag remelting process in the future. Due to using Si_3N_4 as a nitrogen alloying source, the silicon contents in the heat No.6 and No.7 ESR ingots were out of the specification range. Even remelting under high pressure, the addition of Si_3N_4 resulted in a boiling effect of the slag due to the formation of lots of nitrogen gas, which disturbed the remelting process, and the current fluctuated greatly. The surface quality of the heat No.6 and No.7 ESR are bad as shown in Fig. 2(a). Fig. 2(b) shows that the good surface quality using FeCrN as a nitrogen alloying source can be obtained.

Table 2. Chemical composition of steels obtained with a pressurized ESR furnace **wt%**

No.	Steel	Cr	Mn	C	Si	S	P	Mo	Ni	O	N
1	18Cr18MnN	20.13	16.51	0.100	0.54	0.012	0.020	—	—	0.0098	1.00
2	22Cr16MnN	21.22	15.92	0.120	0.49	0.003	0.023	—	—	0.0139	1.21
3	18Cr18Mn2MoN	18.34	18.36	0.068	0.50	0.008	0.024	2.13	—	0.0131	0.93
4	18Cr18Mn2MoN	18.56	18.20	0.069	0.48	0.009	0.025	2.20	—	0.0129	0.93
5	P2000	17.06	13.18	0.042	0.75	0.009	0.021	3.37	—	0.0137	0.79
6	P2000	16.83	13.52	0.045	1.61	0.011	0.022	3.26	—	0.0128	0.78
7	P2000	16.62	13.65	0.042	1.88	0.005	0.024	3.13	—	0.0047	0.63
8	23Cr2Mo4NiN	21.33	—	0.026	0.72	0.010	0.019	2.05	4.00	0.0180	0.88

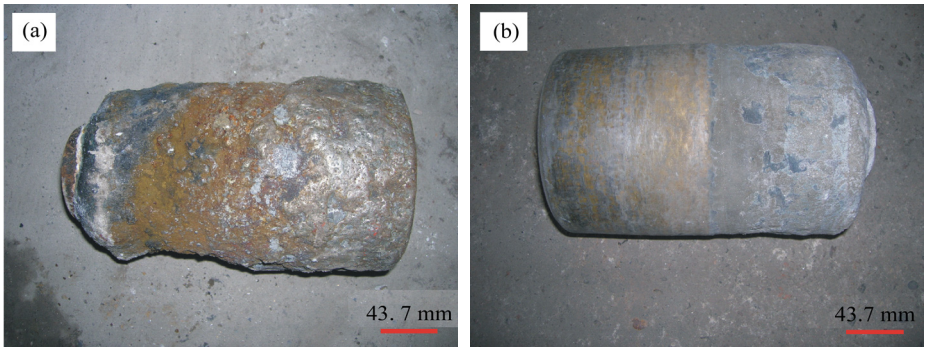

Fig. 2. Appearances of ESR ingots manufactured with a pressurized ESR furnace: (a) the heat No.7; (b) the heat No.2.

Nitrogen was also homogeneously distributed in ESR ingots except for the heat No.1 as shown in Table 3. The bottom nitrogen content in the heat No.1 was lower due to the arc starting and formation of liquid slags under normal atmosphere. There were nonmetallic inclusions with the size less than 5 μm such as Al_2O_3, MnS, and complex inclusions composed of MnS and TiN in the ESR ingots. Fig. 3 shows the typical macrostructures in the longitudinal and transversal directions of an ESR ingot. The ingot was free of all defects.

3.2. Mechanical properties of high nitrogen steels

Table 4 shows the tensile properties of the 18Cr18Mn2Mo0.9N at different crosshead speeds at RT. The results showed that the steel exhibited high tensile strength and good ductility at RT. When increasing the crosshead speed, the tensile strength, elongation, and reduction of area decreased, but the yield strength increased.

Table 3. Nitrogen distribution in ESR ingots in different positions **wt%**

No.	Top		Middle		Bottom	
	N	O	N	O	N	O
1	1.01	0.0086	0.98	0.0099	0.86	0.0150
6	0.77	0.0110	0.77	0.0139	0.76	0.0134
8	0.86	0.0200	0.88	0.0179	0.87	0.0183

The impact absorbed energy of 18Cr18Mn2Mo-0.9N in the temperature range of 77 K up to RT is shown in Fig. 4. It showed favorable toughness between 273 K and 290 K. In the range of 203 K to 273 K, the toughness sharply decreased. When the temperature was lower than 203 K, the impact absorbed energy was lower than 40 J, which showed obvious brittleness. The results showing a typical ductile brittle

transition behavior of the steel were consistent with those of earlier reports [10-14].

Fig. 5 shows four fracture morphologies of the tested 18Cr18Mn2Mo0.9N by scanning electron microscopy (SEM). The fracture morphology at RT showed favorable ductility and equiaxial dimples in Fig. 5(a). With decreasing temperature, dimples became shallow and turned to smooth cleavage facets gradually at 233 K in Fig. 5(b). Quasi cleavage, cleavage facets, and dimples existed together at 203 K, which presented more obvious brittleness as shown in Fig. 5(c). Full of smooth cleavage fracture facets and steps at 77 K can be observed in Fig. 5(d), which showed complete brittleness. The change of the fracture morphologies was dimples → shallow dimples → mixture of quasicleavage, cleavage fracture facets, and dimples → cleavage fracture facets with decreasing temperature. The fracture modes of the steel were transgranular and intergranular fractures at 77 K as shown in Fig. 5(d) (marked A and B, respectively). Cracks along the annealing twin boundary and along (111) γ plane were shown in Fig. 6 (marked C and D), which were found by some researchers [10-12]. Fracture along annealing twin plane [12] also exited on the fracture surfaces at 77 K as shown in Fig. 7. Therefore, in face centered cubic (fcc) structural materials with low stacking fault energy, the feature of fracturing along the annealing twin plane can be used to explain the fracture mechanism [13].

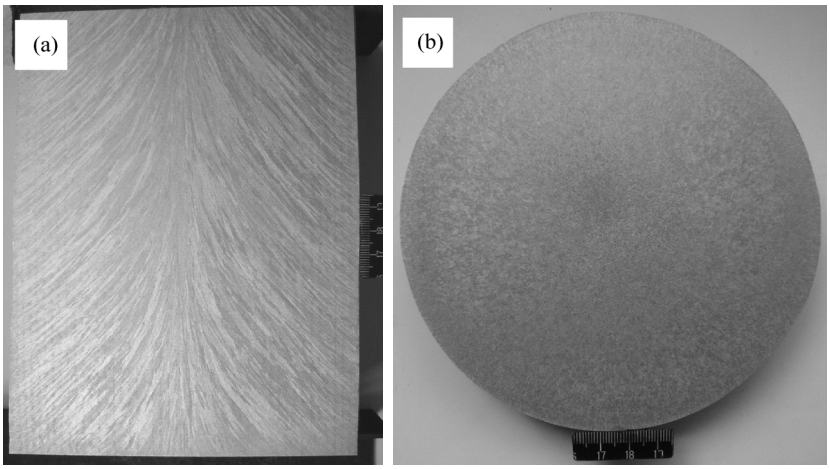

Fig. 3. Macrostructures of an ESR ingot: (a) longitudinal direction; (b) transversal direction.

Table 4. Tensile properties of 18Cr18Mn2Mo0.9N at different crosshead speeds at RT

Crosshead speed / (mm·min^{-1})	Tensile strength / MPa	Yield strength / MPa	Elongation / %	Reduction of area / %
0.5	975	500	62	54
3.0	935	518	60	52
40.0	895	566	50	49

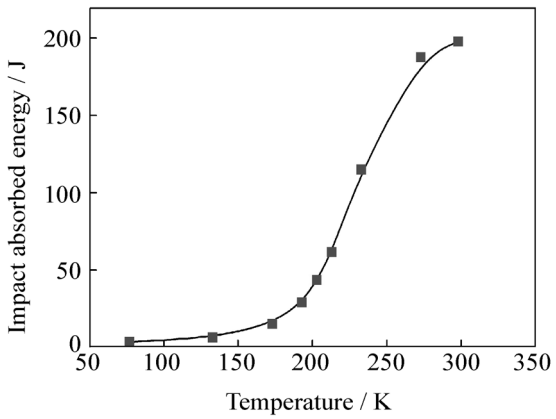

Fig. 4. Impact absorbed energy of 18Cr18Mn2Mo0.9N in the temperature range of 77 K up to RT.

3.3. Pitting corrosion resistance of high nitrogen steels

The anodic polarization curves of 18Cr18Mn2Mo-0.9N high nitrogen austenitic stainless steel and 316L stainless steel in the 3.5wt% NaCl solutions with pH values ranging from 1 to 5 are shown in Fig. 8. It could be seen that there were a wider passive region of all curves of 18Cr18Mn2Mo0.9N compared with that of 316L stainless steel, and the passive region increased with increasing the pH value of the solution. The occurrence of secondary passivation behavior was observed in 3.5wt% NaCl with pH 3.08. The pitting corrosion potential of 18Cr18Mn2Mo did not decrease greatly with decreasing the pH of the solution, and the pitting potential of the steel in the solution with pH = 1 was about 0.8 V. The pitting corrosion potentials of 18Cr18Mn2Mo0.9N in the solution with all pH values were higher than that of 316L, which indicated that 18Cr18Mn2MoN0.9N had more excellent pitting corrosion resistance than 316L. The results showed that

the stability of the passive film against pitting corrosion increased with increasing the pH of the solution. The enriched nitrogen in the passive film of high nitrogen austenitic steel was dissolved and combined with hydrogen ions in the solution to form ammonium ions, which resulted in increasing the pH of the local solution, improved the repassivation, and increased the pitting potential of the steel [15].

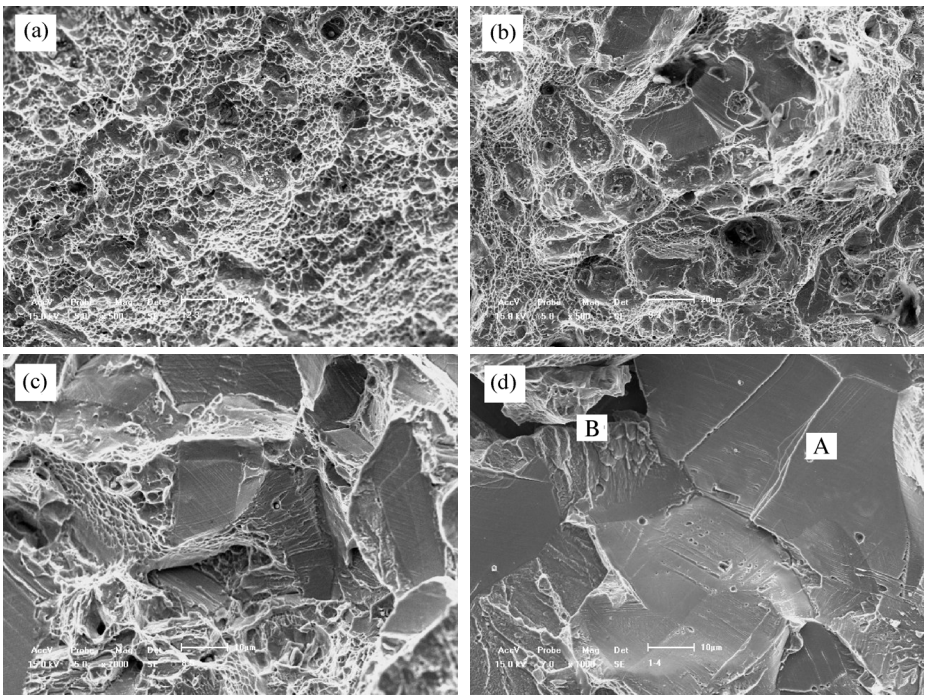

Fig. 5. Impact fracture facets at (a) 290 K, (b) 233 K, (c) 203 K, and (d) 77 K.

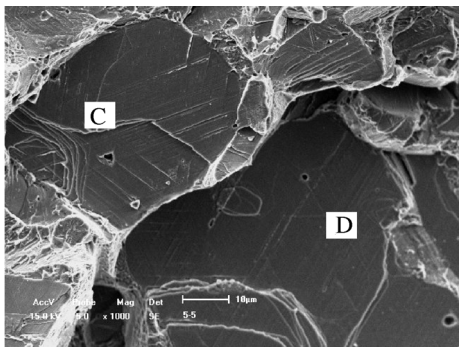

Fig. 6. Crack along the annealing twin boundary (C) and along (111) γ plane (D) at 193 K.

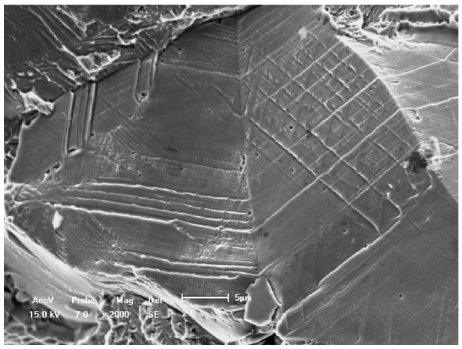

Fig. 7. Fracture along the annealing twin plane at 77

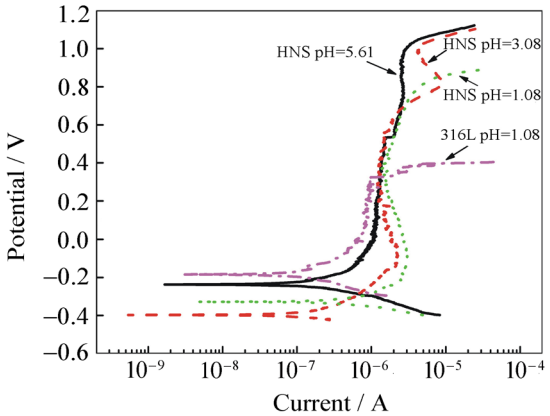

Fig. 8. Anodic polarization curves of 18Cr18Mn2Mo0.9N (HNS) and 316L steel in NaCl solutions with different pH values.

4. Conclusions

(1) A series of high nitrogen austenitic stainless steels have been successfully manufactured by pressurizing with the maximum nitrogen pressure of 7 MPa. The effect of nitrogen alloying using an FeCrN alloy is superior to that of using a Si_3N_4 source under high nitrogen pressure. The sound and compact macrostructure ingot with the maximum nitrogen content of 1.21wt% can be obtained.

(2) The 18Cr18Mn2Mo0.9N high nitrogen austenitic stainless steel made with a pressurized electro-slag remelting furnace exhibits high strength and good ductility at RT. The steel shows typical ductile brittle transition behavior.

(3) 18Cr18Mn2Mo0.9N in 3.5wt % NaCl solutions with pH values ranging from 1 to 5 has excellent pitting corrosion resistance compared with 316L stainless steel. With decreasing the pH value of the solution, the pitting potential of the steel decreases a little.

References

[1] J.W. Simmons, High-nitrogen alloying of stainless steels, *Mater. Sci. Eng. A*, 207(1996), No.2, p.159.

[2] Y. Katada, M. Sagara, Y. Kobayashi, *et al.*, Fabrication of high strength high nitrogen stainless steel with excellent corrosion resistance and its mechanical properties, *Mater. Manuf. Processes*, 19(2004), No.1, p.19.

[3] H.B. Li, Z.H. Jiang, M.H. Shen, *et al.*, Manufacturing high nitrogen austenitic stainless steels by nitrogen gas alloying and adding nitrided ferroalloys, *J. Iron. Steel. Res. Int.*, 14(2007), No.3, p.63.

[4] Y.P. Lang and X.F. Kang, Corrosion resistance of high nitrogen superaustenitic stainless steel and influence of nitrogen, *J. Iron. Steel. Res.* (in Chinese), 13(2001), No.1, p.30.

[5] Y.B. Ren, K. Yang, B.C. Zhang, *et al.*, Nickel-free stainless steel for medical application, *J. Mater. Sci. Technol.*, 20(2004), No.5, p.571.

[6] D.W. Cui, J.S. Jiang, G.M. Cao, *et al.*, Preparation of high nitrogen and nickel-free austenitic stainless steel by power injection molding, *J. Univ. Sci. Tecnol. Beijing*, 15(2008), No.2, p.150.

[7] X. Zhang, C.X. Wang, X.M. Liu, *et al*., Microstructure evolution and mechanical hardening of 18-18-0.5N high-nitrogen austenitic stainless steel during cold rolling, *J. Univ. Sci. Tecnol. Beijing* (in Chinese), 30(2008), No.8, p.875.

[8] D.W. Cui, X.H. Qu, P. Guo, *et al*., Sintering of nickel-free high nitrogen 0Cr17Mn11Mo3N stainless steel prepared by powder injection molding, *J. Univ. Sci. Tecnol. Beijing* (in Chinese), 30(2008), No.10, p.1112.

[9] G. Stein, J. Menzel, and A. Choudhury, Industrial manufacture of massively nitrogen-alloyed steels in a pressure ESR furnace, *Steel Times Int.*, 217(1989), No.3, p.147.

[10] S.C. Liu, T. Hakano, H. Takahashi, *et al.*, A study on fractography in the low-temperature brittle fracture of an 18Cr-18Mn-0.7N austenitic steel, *Metall. Mater. Trans. A*, 29(1998), No.3, p.791.

[11] R.L. Tobler and D. Meyn, Cleavage-like fracture along slip planes in Fe-18Cr-3Ni-13Mn-0.37N austenitic stainless steel at liquid helium temperature, *Metall. Trans. A*, 19(1988), No.6, p.1626.

[12] Y. Tomota and S. Endo, Cleave-like fracture at low temperatures in an 18Mn-18Cr-0.5N austenitic steels, *ISIJ Int.*, 30(1990), No.8, p.656.

[13] H.B. Li, Z.H. Jiang, Z.R. Zhang, *et al.*, Research on fracture behavior of high nitrogen austenitic stainless steels at cryogenic temperature, [in] *Proceedings of Sino-Swedish Structural Materials Symposium 2007*, Beijing, 2007, p.325.

[14] K.M. Chen and Q.X. Dai, Crystallographic features of deformed microstructure in austenitic steel with high N content, *J. Iron. Steel. Res.* (in Chinese), 10(1998), No.1, p.38.

[15] G. Lothongkum, P. Wongpanya, S. Morito, *et al.*, Effect of nitrogen on corrosion behavior of 28Cr-7Ni duplex and microduplex stainless steels in air-saturated 3.5%NaCl solution, *Corros. Sci.*, 48(2006), No.1, p.137.